

FISHER SCORING ALGORITHM FOR TIME-DELAY AND DOPPLER ESTIMATION

Samuele Alteri¹, Samy Labsir^{1,2}, Lorenzo Ortega^{1,2}

¹ TéSA laboratory, Toulouse, France,

^{1,2} Institut Polytechnique des Sciences Avancées, Toulouse, France

ABSTRACT

Time-delay and Doppler estimation are among the most critical operations for synchronizing wireless communication systems, as well as for applications such as radar and global navigation satellite system (GNSS). Typically, a maximum likelihood estimator (MLE) is employed to initialize the time-delay and Doppler parameters. However, due to the high computational complexity of the MLE, sub-optimal algorithms are often used for subsequent parameter tracking. In this paper, we propose a novel low-complexity Fisher-scoring estimator, which is a variant of the Newton-Raphson method. Under the band-limited assumption, we derive closed-form expressions for the Fisher Information Matrix (FIM) and the gradient, both of which depend solely on the received signal samples. The performance of the proposed estimator is evaluated against the Cramér-Rao Bound (CRB), demonstrating asymptotic convergence and achieving the same performance as the MLE after a certain number of iterations.

Index Terms— Time-delay and Doppler estimation, Fisher-scoring method, band limited signal.

1. INTRODUCTION

In the context of digital communication systems, accurately estimating the parameters of the received signal is essential. These parameters—typically the time-delay and Doppler frequency—carry information about the position and velocity of the signal source. Such estimates enable a variety of signal processing tasks, including target tracking and classification. [1–10]. In the current state of the art, a variety of methodologies have been explored to achieve precise time-delay and Doppler estimation, including non-parametric approaches such as correlation-based techniques and subspace methods, as well as parametric approaches based on the maximum likelihood estimation (MLE) [2, 11]. While correlation-based methods are straightforward and computationally efficient, they often underperform in low signal-to-noise ratio (SNR) conditions and lack the precision required in high-accuracy applications. Subspace methods, such as MUSIC and ESPRIT [2], improve accuracy by exploiting the separation between signal and noise subspaces, but they may suffer from computational complexity and limitations in dynamic or wideband signal scenarios [12]. The MLE, while optimal only under linear Gaussian signal model assumptions, it has been shown to be asymptotically efficient under the conditional signal model (CSM) [13], delivering high estimation accuracy when the signal-to-noise ratio (SNR) is sufficiently high [14]. Additionally, since MLE is based on a parametric model and asymptotically unbiased, it is possible to quantify the accuracy of the Mean Squared Error (MSE) through the well-known Cramér-Rao bound (CRB) [11]. In our work, we propose to focus on this method. It is important to emphasize that it does not admit an analytical solution, and has to

be computed using a numerical technique. The simplest idea consists in implementing a grid-search approach to determine the point that maximizes the likelihood [15–17]. It generally provides high accuracy in terms of precision, but it is very costly in terms of computation, particularly in diverse contexts where parameters need to be iteratively updated over time. To address this issue and reduce the cost, we can resort to optimization algorithms based on descent direction. However, for generic estimation problems, Newton-based techniques have some limitations, especially due to the need for analytical computations and the inversion of the Hessian matrix. Optimization techniques such as the Fisher-Scoring (FS) method have emerged as practical alternatives, leveraging the computation of the Fisher Information Matrix (FIM) to approximate the Hessian matrix. The FS method has demonstrated its effectiveness in related estimation contexts, such as image restoration—where it is applied to determine blur coefficients [18]—and in model parameter estimation for Direction-Of-Arrival (DOA) tasks in seismic arrays. Note that for the same application, a modified version of FS known as the periodic Fisher-Scoring approach, has been proposed and adapted to estimate phase information [19]. The main contribution of this paper is to adapt the FS algorithm for the joint estimation of time-delay and Doppler parameters from received signals in wireless communication. To this end, we derive a novel closed-form expression for the gradient of the maximum likelihood (ML) criterion, under the assumption of Gaussian noise and band-limited received signals. To the best of our knowledge, this expression has not been derived in the existing literature. As for the FIM, we rely on its closed-form expression, first derived in [15]. A key advantage of the FIM—compared to the Hessian matrix required in Newton-based methods—is that it does not depend on the current parameter estimates, resulting in a significant reduction in computational complexity. The performance of the proposed method is assessed through a series of numerical experiments. The MSE of the time-delay and Doppler estimates is compared to that obtained via a grid-search-based ML estimator. Furthermore, the accuracy of the method is evaluated with respect to the CRB. The letter is organized as follows: Section 2.1, we introduce the signal model. In Sections 2.2, we present the problem, by introducing the signal model, CRB and MLE under the band-limited signal assumption. In Section 3, we describe the proposed FS algorithm. In Section 4, we present numerical results that validate the good performance of the proposed algorithm. Finally, the main findings and contributions of the paper are summarized in Section 5.

2. PROBLEM FORMULATION

2.1. Signal model

Consider a wireless communication system in which a band-limited signal $a(t)$, with bandwidth B , is transmitted over a carrier frequency f_c from a transmitter located at position $\mathbf{p}_{T_X}(t)$ to a

receiver at position $\mathbf{p}_{R_X}(t)$. Under the band-limited signal assumption, $a(t)$ can be expressed as:

$$a(t) = \sum_{n=N_1}^{N_2} a(nT_s) \text{sinc}(\pi B(t - nT_s)) \Leftrightarrow$$

$$a(f) = \left(\frac{1}{F_s} \sum_{n=N_1}^{N_2} a(nT_s) e^{-j2\pi f nT_s} \right) \mathbf{1}_{[-\frac{F_s}{2}; \frac{F_s}{2}]}, \quad (1)$$

where $T_s = \frac{1}{B} = \frac{1}{F_s}$ is the sampling period and F_s is the sampling frequency. The distance traveled by the transmitted signal can be approximated by a first order as

$$\mathbf{p}_{(Tx, Rx)}(t) = \|\mathbf{p}_{Tx}(t - \tau_0(t)) - \mathbf{p}_{Rx}(t)\| \approx \bar{\tau} + \bar{b}t, \quad (2)$$

with $\bar{\tau} = \frac{\|\mathbf{p}_{Tx}(0) - \mathbf{p}_{Rx}(0)\|}{c}$, $\bar{b} = \frac{\|\mathbf{v}\|}{c}$, and \mathbf{v} the relative velocity between transmitter and receiver. The received signal after baseband demodulation can be expressed as [15]

$$x(t) = \bar{\alpha} a((t - \bar{\tau})(1 - \bar{b})) e^{-j2\pi f_c(\bar{b}(t - \bar{\tau}))} + n(t), \quad (3)$$

which simplifies under the narrowband assumption to [20]

$$x(t) = \bar{\alpha} a(t - \bar{\tau}) e^{-j2\pi f_c(\bar{b}(t - \bar{\tau}))} + n(t), \quad (4)$$

with $\bar{\alpha} = \bar{\rho} e^{j\bar{\Phi}}$ a complex gain defined as $\bar{\rho} \in \mathbb{R}^+$, $0 \leq \bar{\Phi} \leq 2\pi$, and $n(t)$ a zero-mean, Gaussian wide-sense stationary noise process. After completing the sampling operation, the discrete signal model with $N = |N_1 - N_2 + 1|$ samples at sampling rate T_s can be expressed as:

$$\mathbf{x} = \bar{\alpha} \boldsymbol{\mu}(\bar{\boldsymbol{\eta}}) + \mathbf{n}, \quad (5)$$

where $\mathbf{n} \in \mathbb{C}^N$ is distributed as a centered circular complex normal vector with diagonal covariance matrix, i.e. $\mathbf{n} \sim \mathcal{CN}(\mathbf{0}, \bar{\sigma}^2 \mathbf{I}_N)$, $\mathbf{x} = (\dots, x_k, \dots) = (\dots, x(kT_s; \bar{\boldsymbol{\eta}}), \dots)^\top$ for $N_1 \leq k \leq N_2$ and $\bar{\boldsymbol{\eta}} = [\bar{\tau}, \bar{b}]^\top$. Finally, we have

$$\boldsymbol{\mu}(\bar{\boldsymbol{\eta}}) = (\dots, \mu_k, \dots) = (\dots, a(kT_s - \bar{\tau}) e^{-j2\pi f_c(\bar{b}(kT_s - \bar{\tau}))}, \dots)^\top. \quad (6)$$

In expression (5), we identify the vector of unknown parameter denoted as $\bar{\boldsymbol{\epsilon}}^\top = (\bar{\sigma}^2, \bar{\rho}, \bar{\Phi}, \bar{\boldsymbol{\eta}}^\top) = (\bar{\sigma}^2, \bar{\boldsymbol{\theta}}^\top)$.

2.2. Closed-form CRB expression for band-limited signals

It is noteworthy that a closed-form expression of the CRB was previously derived in the literature [13]. More recently, a compact form of the corresponding FIM, depending solely on the baseband signal samples, was derived in [15, 16] as follows:

$$\text{FIM}(\bar{\boldsymbol{\theta}}) = \frac{2F_s}{\bar{\sigma}^2} \Re \left\{ \mathbf{Q} \mathbf{W} \mathbf{Q}^H \right\}, \quad (7)$$

with

$$\mathbf{W} = \begin{bmatrix} w_1 & w_2^* & w_3^* \\ w_2 & W_{2,2} & w_4^* \\ w_3 & w_4 & W_{3,3} \end{bmatrix}, \quad (8a)$$

$$\mathbf{Q} = \begin{bmatrix} 1 & 0 & 0 \\ j\bar{\rho} & 0 & 0 \\ j\bar{\rho} 2\pi f_c \bar{b} & 0 & -\bar{\rho} \\ 0 & -j\bar{\rho} 2\pi f_c & 0 \end{bmatrix}, \quad (8b)$$

where the entries of \mathbf{W} can be represented with respect to the baseband signal samples as follows:

$$w_1 = \frac{1}{F_s} \mathbf{a}^H \mathbf{a}, \quad w_2 = \frac{1}{F_s^2} \mathbf{a}^H \mathbf{D} \mathbf{a}, \quad w_3 = \mathbf{a}^H \boldsymbol{\Lambda} \mathbf{a}, \quad (9)$$

$$w_4 = \frac{1}{F_s} \mathbf{a}^H \mathbf{D} \boldsymbol{\Lambda} \mathbf{a}, \quad W_{2,2} = \frac{1}{F_s^3} \mathbf{a}^H \mathbf{D}^2 \mathbf{a}, \quad W_{3,3} = F_s \mathbf{a}^H \mathbf{V} \mathbf{a},$$

with

$$\mathbf{D} = \text{diag}(\dots, k, \dots)_{N_1 \leq k \leq N_2}, \quad (10a)$$

$$(\boldsymbol{\Lambda})_{k,k'} = \begin{cases} k' \neq k : \frac{(-1)^{|k-k'|}}{k-k'} \\ k' = k : 0 \end{cases}, \quad (10b)$$

$$(\mathbf{V})_{k,k'} = \begin{cases} k' \neq k : \frac{(-1)^{|k-k'|}}{(k-k')^2} \\ k' = k : \frac{\pi^2}{3} \end{cases}. \quad (10c)$$

2.3. MLE estimator

The MLE involves finding the parameter $\boldsymbol{\epsilon}$ that maximizes the log-likelihood associated with the model (5). The resulting estimator $\hat{\boldsymbol{\theta}}$ is an asymptotically efficient estimate of $\bar{\boldsymbol{\theta}}$ and can be expressed as [15, 21]¹:

$$\hat{\boldsymbol{\eta}} = \arg \max_{\boldsymbol{\eta}} \|\boldsymbol{\Pi} \boldsymbol{\mu}(\boldsymbol{\eta}) \mathbf{x}\|^2 \quad (11)$$

$$\hat{\rho} = \left| \left[\boldsymbol{\mu}^H(\hat{\boldsymbol{\eta}}) \boldsymbol{\mu}(\hat{\boldsymbol{\eta}}) \right]^{-1} \boldsymbol{\mu}^H(\hat{\boldsymbol{\eta}}) \mathbf{x} \right| \quad (12)$$

$$\hat{\Phi} = \arg \left\{ \left[\boldsymbol{\mu}^H(\hat{\boldsymbol{\eta}}) \boldsymbol{\mu}(\hat{\boldsymbol{\eta}}) \right]^{-1} \boldsymbol{\mu}^H(\hat{\boldsymbol{\eta}}) \mathbf{x} \right\}. \quad (13)$$

Due to the complexity of the criterion, obtaining a closed-form expression for $\boldsymbol{\eta}$ is not feasible. As a result, numerical approaches are required. Grid-based search techniques are generally performed because they offer high precision, but they are computationally expensive—particularly in dynamic scenarios where the solution must be updated recursively. Thus, it is crucial to design an algorithm bypassing this computational cost.

3. FISHER SCORING ALGORITHM FOR TIME-DELAY AND DOPPLER ESTIMATION

In this section, we present the main contribution of this work: the design of a Fisher Scoring algorithm for parameter estimation based on the ML approach, leveraging the properties of band-limited signals.

3.1. Algorithm design

Traditionally, descent-based algorithms can be used to solve the log-likelihood equation. However, gradient-based methods are not well-suited for our problem due to their sensitivity to noise and slow convergence, especially when working with noisy signals or when the likelihood functions are not smooth. In this work, we propose focusing on the FS method, which is a modified form of the Newton-Raphson method. Instead of using the Hessian matrix (the second derivatives of the log-likelihood), the FS method replaces it with the FIM, which is its expected value. The recursion at each iteration i of the FS algorithm can be expressed as follows:

$$\hat{\boldsymbol{\theta}}_{i+1} = \hat{\boldsymbol{\theta}}_i + \text{FIM}^{-1}(\hat{\boldsymbol{\theta}}_i) \nabla \mathbf{x}(\hat{\boldsymbol{\theta}}_i), \quad (14)$$

¹Let $S = \text{span}(\mathbf{A})$, with \mathbf{A} a matrix, be the linear span of the set of its column vectors. The orthogonal projector over S is $\boldsymbol{\Pi}_A = \mathbf{A} (\mathbf{A}^H \mathbf{A})^{-1} \mathbf{A}^H$.

where $\hat{\boldsymbol{\theta}}_i^T = (\rho_i, \phi_i, \boldsymbol{\eta}_i^T)$, $\nabla \mathbf{x}(\hat{\boldsymbol{\theta}}_i)$ is the gradient of the log-likelihood associated with the signal model in (5). The initial guess $\hat{\boldsymbol{\theta}}_0$ must be close to the true value, so we use the output of the MLE provided by equations (11), (12), and (13) as the initialization. This operation is performed only one time during initialization, which significantly reduces the computational complexity compared to repeatedly applying the MLE with grid-based search.

3.2. Closed-forms expression of the gradient and the FIM

In the following, we propose to compute a closed-form expression of the expression in (14). To achieve this, we observe that (7) provides a closed-form expression of the FIM that depends only on the signal samples and $\hat{\boldsymbol{\theta}}_i$. Then, we can compute FIM ($\hat{\boldsymbol{\theta}}_i$) as follows

$$\text{FIM}(\hat{\boldsymbol{\theta}}_i) = \frac{2F_s}{\hat{\sigma}_i^2} \Re \left\{ \mathbf{Q}_i \mathbf{W} \mathbf{Q}_i^H \right\}, \quad (15)$$

with \mathbf{Q}_i , denoting equation (8) evaluated using the estimates $\hat{\boldsymbol{\theta}}_i$. Moreover, the current estimation of noise variance $\hat{\sigma}_i^2$ can be computed from the MLE expression which is given by:

$$\hat{\sigma}_i^2 = \frac{1}{N} \|\mathbf{x} - \hat{\rho}_i e^{j\hat{\Phi}_i} \boldsymbol{\mu}(\hat{\boldsymbol{\eta}}_i)\|^2. \quad (16)$$

The next step is to calculate the gradient $\nabla \mathbf{x}(\hat{\boldsymbol{\theta}}_i)$, applying the derivative with respect to $\bar{\boldsymbol{\theta}}$ of the criterion:

$$\nabla \mathbf{x}(\hat{\boldsymbol{\theta}}_i) = \frac{2}{\hat{\sigma}_i^2} \sum_{k=N_1}^{N_2} \Re \left\{ u_k^* \left(\frac{\partial \hat{\rho}_i e^{j\hat{\Phi}_i} \mu_k(\hat{\boldsymbol{\eta}}_i)}{\partial \bar{\boldsymbol{\theta}}} \right) \right\} \quad (17)$$

with $u_k = (x_k - \hat{\rho}_i e^{j\hat{\Phi}_i} \mu_k(\hat{\boldsymbol{\eta}}_i))$ and

$$\left(\frac{\partial \hat{\rho}_i e^{j\hat{\Phi}_i} \mu_k(\hat{\boldsymbol{\eta}}_i)}{\partial \bar{\boldsymbol{\theta}}} \right)^T = e^{j\hat{\Phi}_i} \mathbf{Q}_i \boldsymbol{\vartheta}(kT_s; \hat{\boldsymbol{\theta}}_i) e^{-j\omega_c \hat{b}_i(kT_s - \hat{\tau}_i)}, \quad (18)$$

with $\boldsymbol{\vartheta}(t; \hat{\boldsymbol{\theta}}_i) = \begin{bmatrix} a(t - \hat{\tau}_i) \\ (t - \hat{\tau}_i)a(t - \hat{\tau}_i) \\ a^{(1)}(t - \hat{\tau}_i) \end{bmatrix}$, $w_c = 2\pi f_c$ and $a^{(1)}(t) =$

$\frac{\partial a(t)}{\partial t}$. The challenge here is to compute a closed-form expression for the derivative of $a(t)$ in the discrete-time domain. To address this, we rely on the band-limited signal assumption and apply the Nyquist-Shannon sampling theorem, which allows us to reconstruct a continuous-time signal from its samples, as done in previous works [15, 21, 22], then

$$\begin{aligned} & \lim_{(N_1, N_2) \rightarrow (-\infty, \infty)} \left(\sum_{k=N_1}^{N_2} u_k^* \boldsymbol{\vartheta}(kT_s; \boldsymbol{\theta}) e^{-j\omega_c b(kT_s - \tau)} \right) \\ &= F_s \int_{-\infty}^{\infty} u^*(t) \boldsymbol{\vartheta}(t; \boldsymbol{\theta}) e^{-j\omega_c b(t - \tau)} dt = \mathbf{w}_e. \end{aligned} \quad (19)$$

Note that $\mathbf{w}_e^T = (w_{e1}, w_{e2}, w_{e3})$ can be computed following the approach proposed in [23]. This involves applying Parseval's theorem, which allows the computation of a time-domain derivative as a simple multiplication in the Fourier domain. Then, leveraging the band-limited signal assumption and the Nyquist-Shannon sampling theorem, the result can be transformed from the frequency domain to the discrete-time domain, reducing the integral in (19) to simple matrix products.

$$\begin{aligned} w_{e1} &= F_s \int_{-\infty}^{\infty} u^*(t) a(t - \tau) e^{-j\omega_c b(t - \tau)} dt \\ &= \int_{-\infty}^{\infty} u^*(t + \tau) a(t) e^{-j\omega_c b t} dt \\ &= \int_{-\frac{F_s}{2}}^{\frac{F_s}{2}} U^*(f) A(f - f_c b) e^{j2\pi f \tau} df \\ &= \mathbf{u}^H \mathbf{V}^{\Delta, 0} \left(\frac{\tau}{T_s} \right) \mathbf{U} \left(\frac{f_c b}{F_s} \right) \mathbf{a}, \end{aligned} \quad (20)$$

$$\begin{aligned} w_{e2} &= F_s \int_{-\infty}^{\infty} (t - \tau) a(t - \tau) u^*(t) e^{-j\omega_c b(t - \tau)} dt \\ &= F_s \int_{-\infty}^{\infty} t a(t) u^*(t + \tau) e^{-j\omega_c b t} dt \\ &= F_s \int_{-\frac{F_s}{2}}^{\frac{F_s}{2}} \frac{j}{2\pi} \frac{d}{df} \left(U^*(f) e^{-j2\pi f \tau} \right) \cdot (A(f - f_c b)) df \\ &= \frac{1}{F_s} \mathbf{u}^H \mathbf{V}^{\Delta, 0} \left(\frac{\tau}{T_s} \right) \mathbf{U} \left(\frac{f_c b}{F_s} \right) \mathbf{D} \mathbf{a}, \end{aligned} \quad (21)$$

$$\begin{aligned} w_{e3} &= F_s \int_{-\infty}^{\infty} a^{(1)}(t - \tau) u^*(t) e^{-j\omega_c b(t - \tau)} dt \\ &= F_s \int_{-\infty}^{\infty} a^{(1)}(t) u^*(t + \tau) e^{-j\omega_c b t} dt \\ &= F_s \int_{-\frac{F_s}{2}}^{\frac{F_s}{2}} \frac{j}{2\pi} \frac{d}{df} \left(U^*(f) e^{-j2\pi f \tau} \right) A(f - f_c b) df \\ &= F_s \mathbf{u}^H \mathbf{V}^{\Delta, 1} \left(\frac{\tau}{T_s} \right) \mathbf{U} \left(\frac{f_c b}{F_s} \right) \mathbf{a} + \\ & \quad j\omega_c b \mathbf{u}^H \mathbf{V}^{\Delta, 0} \left(\frac{\tau}{T_s} \right) \mathbf{U} \left(\frac{f_c b}{F_s} \right) \mathbf{a}, \end{aligned} \quad (22)$$

with $\mathbf{u} = (\dots, u(kT_s), \dots)^T$ and

$$\mathbf{U}(p) = \text{diag}(\dots, e^{-j2\pi p k}, \dots)_{N_1 \leq k \leq N_2}, \quad (23)$$

$$\left(\mathbf{V}^{\Delta, 0}(q) \right)_{k,l} = \text{sinc}(k - l - q), \quad (24)$$

$$\left(\mathbf{V}^{\Delta, 1}(q) \right)_{k,l} = \frac{1}{k - l - q} (\cos(\pi(k - l - q)) - \text{sinc}(k - l - q)). \quad (25)$$

Note that (17) yields to

$$\nabla \mathbf{x}(\hat{\boldsymbol{\theta}}_i) = \frac{2}{\hat{\sigma}_i^2} \Re \left\{ e^{j\hat{\Phi}_i} \mathbf{Q}_i \mathbf{w}_{e,i} \right\} \quad (26)$$

with $\mathbf{w}_{e,i} = F_s \int_{-\infty}^{\infty} u^*(t) \boldsymbol{\vartheta}(t; \hat{\boldsymbol{\theta}}_i) e^{-j\omega_c \hat{b}_i(t - \hat{\tau}_i)} dt$ and therefore we can express the closed-form expression for our FS algorithm as

$$\hat{\boldsymbol{\theta}}_{i+1} = \hat{\boldsymbol{\theta}}_i + T_s \Re \left\{ \mathbf{Q}_i \mathbf{W} \mathbf{Q}_i^H \right\}^{-1} \Re \left\{ e^{j\hat{\Phi}_i} \mathbf{Q}_i \mathbf{w}_{e,i} \right\}. \quad (27)$$

Several points justify the algorithm's low complexity. First, given the structure of equation (14) and the expressions in (15) and (17), we note that variance estimation in (16) is not required to be computed. Second, while computing the \mathbf{W} matrix is more computationally intensive operation in this algorithm, it is independent of the estimation parameters and can therefore be precomputed offline once the integration time and sampling frequency parameters are set. Finally, equations (20)-(22) can be computed efficiently since \mathbf{U} and \mathbf{D} are diagonal matrices, and the product of \mathbf{u} and \mathbf{V} can be computed using the FFT domain, since \mathbf{V} is a circular matrix.

4. NUMERICAL RESULTS AND DISCUSSION

In this section, it is validated the performance of the proposed FS algorithm in a satellite navigation context. Specifically, we examine a scenario where a GPS L1 C/A signal [10] is received by a GNSS receiver. The analysis assumes a setup where the GNSS receiver operate with a sampling frequency $F_s = 4\text{MHz}$ and an integration time of 1 ms. The Doppler frequency is set to 500 Hz. Within 1 ms interval, the GPS L1 C/A signal consists of a Gold code (pseudorandom code) with 1023 chips. To evaluate the root mean square error (RMSE) \sqrt{MSE} of the proposed FS estimator, we conduct a simulation based on 1000 Monte Carlo runs. Furthermore, the RMSE is analyzed as a function of the signal-to-noise ratio (SNR) at the output of the match filter, which is defined as:

$$SNR_{out} = \frac{|\bar{\alpha}|^2 \mathbf{a}^H \mathbf{a}}{\bar{\sigma}_n^2}. \quad (28)$$

Figures 1 and 2 show the RMSE of the time-delay and Doppler estimation of the Fisher-scoring algorithm for $i = \{1, 5, 10\}$ iterations as well as the RMSE for the MLE with grid-based search. Moreover the CRB is included in both figures to show the theoretical estimation limit for unbiased estimators. The range of SNR_{out} values has been selected consistently with the operational SNR range of the GPS system. The initialization of the FS algorithm for its first iteration is set to the output value of the MLE estimator. Several interesting points can be observed: i) the FS algorithm with a single iteration performs better than the MLE up to 35 dB of SNR_{out} ; beyond this SNR range, a bias appears. This is consistent with the theory since the RMSE of a biased algorithm can be lower than the CRB for some SNR intervals. ii) When using 5 or 10 iterations, it can be observed that the FS algorithm converges to the CRB. The higher the number of iterations, the faster the convergence. Nevertheless, before convergence, the algorithm performs better than the MLE. This is because the algorithm with 5 or 10 iterations remains biased, however, the bias appears at SNR levels much higher than those shown in the graphs (and beyond the operational range of the GPS system).

5. CONCLUSIONS

In this letter, we derive a closed-form expression of the FS algorithm for estimating time-delay and Doppler parameters. The FS algorithm offers a significant reduction in computational complexity compared to the MLE, while maintaining robust performance. Simulation results, using the GPS L1 C/A signal, demonstrate that after just one iteration, the FS algorithm is biased but outperforms the MLE up to 35 dB of SNR_{out} . As the number of iterations increases, the FS algorithm converges to the CRB, achieving asymptotic performance equivalent to the MLE within the operational SNR range of the GPS system. Overall, the FS algorithm presents a computationally efficient alternative to the MLE.

6. REFERENCES

- [1] D. A. Swick, "A Review of Wideband Ambiguity Functions," Tech. Rep. 6994, Naval Res. Lab., Washington DC, 1969.
- [2] H. L. Van Trees, *Detection, Estimation, and Modulation Theory, Part III: Radar – Sonar Signal Processing and Gaussian Signals in Noise*, J. Wiley & Sons, 2001.
- [3] U. Mengali and A. N. D'Andrea, *Synchronization Techniques for Digital Receivers*, Plenum Press, New York, USA, 1997.

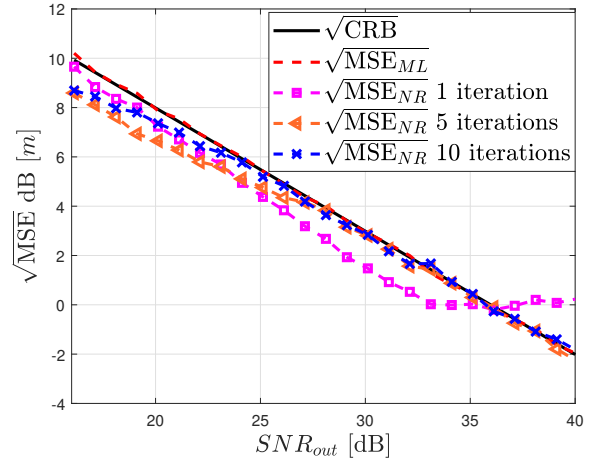


Fig. 1: Time-delay estimation for MLE and FS algorithm with $i = \{1, 5, 10\}$ iterations. F_s is set to 4 MHz.

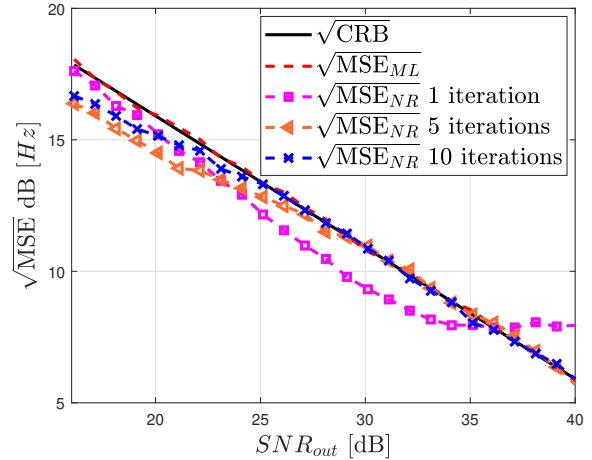


Fig. 2: Doppler estimation for MLE and FS algorithm with $i = \{1, 5, 10\}$ iterations. F_s is set to 4 MHz.

- [4] H. L. Van Trees, *Optimum Array Processing*, Wiley-Interscience, New-York, 2002.
- [5] D. W. Ricker, *Echo Signal Processing*, Kluwer Academic, Springer, New York, USA, 2003.
- [6] J. Chen, Y. Huang, and J. Benesty, "Time delay estimation," in *Audio Signal Processing for Next-Generation Multimedia Communication Systems*, Y. Huang and J. Benesty, Eds., chapter 8, pp. 197–227. Springer, Boston, MA, USA, 2004.
- [7] B. C. Levy, *Principles of Signal Detection and Parameter Estimation*, Springer, 2008.
- [8] F. Bouchereau D. Munoz, C. Vargas, and R. Enriquez, *Position Location Techniques and Applications*, Academic Press, Oxford, GB, 2009.
- [9] J. Yan et al., "Review of range-based positioning algorithms," *IEEE Trans. Aerosp. Electron. Syst.*, vol. 28, no. 8, pp. 2–27, Aug. 2013.

- [10] P. J. G. Teunissen and O. Montenbruck, Eds., *Handbook of Global Navigation Satellite Systems*, Springer, Switzerland, 2017.
- [11] S. M. Kay, *Fundamentals of Statistical Signal Processing: Estimation Theory*, Prentice-Hall, Englewood Cliffs, New Jersey, USA, 1993.
- [12] Jeong-Geun Hong, Chan-Sik Park, and Bo-Seok Seo, "Comparison of music and esprit for direction of arrival estimation of jamming signal," in *2012 IEEE International Instrumentation and Measurement Technology Conference Proceedings*, 2012, pp. 1741–1744.
- [13] P. Stoica and A. Nehorai, "Performances study of conditional and unconditional direction of arrival estimation," *IEEE Trans. Acoust., Speech, Signal Process.*, vol. 38, no. 10, pp. 1783–1795, Oct. 1990.
- [14] A. Renaux, P. Forster, E. Chaumette, and P. Larzabal, "On the high-SNR conditional maximum-likelihood estimator full statistical characterization," *IEEE Trans. Signal Process.*, vol. 54, no. 12, pp. 4840 – 4843, Dec. 2006.
- [15] D. Medina, L. Ortega, J. Vilà-Valls, P. Closas, François Vincent, and E. Chaumette, "Compact CRB for Delay, Doppler, and Phase Estimation – Application to GNSS SPP and RTK Performance Characterisation," *IET Radar, Sonar & Navigation*, vol. 14, no. 10, pp. 1537–1549, 2020.
- [16] C. Lubeigt, L. Ortega, J. Vilà-Valls, L. Lestarquit, and E. Chaumette, "Joint delay-doppler estimation performance in a dual source context," *Remote Sensing*, vol. 12, no. 23, 2020.
- [17] H. McPhee, L. Ortega, J. Vilà-Valls, and E. Chaumette, "Accounting for acceleration—signal parameters estimation performance limits in high dynamics applications," *IEEE Transactions on Aerospace and Electronic Systems*, vol. 59, no. 1, pp. 610–622, 2023.
- [18] Faruk sari and M. Ertugrul Çelebi, "A new trust region fisher scoring optimization for image and blur identification," in *2004 12th European Signal Processing Conference*, 2004, pp. 505–508.
- [19] Malaak Khatib, Yochai Ben-Horin, Yael Radzyner, Jonathan D. Rosenblatt, and Tirza Routtenberg, "Periodic fisher-scoring algorithm with applications for doa estimation in seismic arrays," in *2023 26th International Conference on Information Fusion (FUSION)*, 2023, pp. 1–7.
- [20] A. Dogandzic and A. Nehorai, "Cramér-Rao bounds for estimating range, velocity, and direction with an active array," *IEEE Trans. Signal Process.*, vol. 49, no. 6, pp. 1122–1137, June 2001.
- [21] L. Ortega, C. Lubeigt, J. Vilà-Valls, and E. Chaumette, "On gnss synchronization performance degradation under interference scenarios: Bias and misspecified cramér-rao bounds," *NAVIGATION: Journal of the Institute of Navigation*, vol. 70, no. 4, 2023.
- [22] C. Lubeigt, L. Ortega, J. Vilà-Valls, and E. Chaumette, "Untangling first and second order statistics contributions in multipath scenarios," *Signal Processing*, vol. 205, pp. 108868, 2023.
- [23] C. Lubeigt, L. Ortega, J. Vilà-Valls, and E. Chaumette, "Technical note: Developments for MCRB Computation in Multipath Scenarios," 2022.